Ionics (2006) 12: 7–14
DOI 10.1007/s11581-006-0002-x

ORIGINAL PAPER

S. P. S. Badwal · S. Giddey · F. T. Ciacchi

# Hydrogen and oxygen generation with polymer electrolyte membrane (PEM)-based electrolytic technology

Received: 25 January 2006 / Accepted: 9 February 2006 / Published online: 26 April 2006


**Abstract** With dwindling liquid fuel resources, hydrogen offers a credible alternative. The use of hydrogen in a fuel cell offers the highest fuel conversion efficiency compared with all other technologies and it also has the potential to substantially reduce greenhouse gas and particulate emissions at least at the end-user sites. One of the major barriers to the introduction of the hydrogen economy and its wider acceptance is the lack of the rather costly hydrogen generation, transportation and distribution infrastructure to meet the local transport fuel demands. On-site or distributed hydrogen generation would remove the need for this up-front infrastructure requirements and assist with the early large-scale trials of the fuel cell technology for both transport and stationary applications and also introduction of the hydrogen economy. In this paper, the development of polymer electrolyte membrane electrolysis technology for on-site, on-demand hydrogen generation has been discussed. The major emphasis is given on reducing catalyst cost; interface design and modifications; interconnect materials, design and fabrication; and investigation of the sources of degradation. Stacks to 2 $kW_{H2}$ capacity have been constructed and tested and show initial efficiencies of >87% at 1 A $cm^{-2}$.

**Keywords** Hydrogen production · Electrolysis · Renewable energy · Polymer electrolyte membrane

## Introduction

As fossil fuel and especially liquid fuel reserves start declining and the gap between demand and supply widens, the cost of transport fuels would increase at an alarming rate and there will be an increasing need to find alternative transport fuels. Hydrogen is the cleanest fuel available to mankind but it has to be generated from fossil fuels with inherent embedded energy or from water by supplying energy. Linking of hydrogen generation with renewable energy would provide a totally sustainable energy cycle. However, most renewable sources are intermittent sources of power and require energy storage for load levelling and to reduce overall plant cost. Hydrogen is arguably the best energy storage medium and is an excellent alternative to carbon-based transport fuels.

The current world $H_2$ generation capacity is about 500 billion $m^3$/year=42 million tons/year (=1.6% of the global energy consumption) (90 billion $m^3$/year in the USA) [1]. Most $H_2$ (~95%) is produced from fossil fuels, mainly natural gas. The major uses of hydrogen are:

- Over half of the total hydrogen produced is utilised for ammonia (fertilizer and explosive) production
- About one third in oil refineries—for impurity removal and upgrading of heavy oil fractions into lighter and more valuable products
- Remaining in methanol production, chemical and metallurgical industries and space programs

The use of hydrogen as a power generation source is minimal at this stage due to its high cost of production, lack of hydrogen transport, storage and distribution infrastructure and technological challenges related to production, storage and end-use of hydrogen. The current total global hydrogen production is barely enough to feed the US transport fleet. Global oil production is likely to peak in the next 5–10 years (it has already peaked in Australia, USA and Europe) and soon the world will run short of oil [2–4]. The demand for transport fuels and energy is increasing at an alarming rate especially in developing and heavily populated countries such as India and China. As the gap between supply and demand for liquid fuels increases, oil prices will increase and there will be increasing requirements to use alternative clean and low- or zero-emission fuels such as hydrogen.

Hydrogen is considered to be the best energy storage media due to its flexibility for end-use and regenerative and zero-emission properties. Hydrogen combusted in a fuel cell can give combined heat and power efficiencies of more

S. P. S. Badwal (✉) · S. Giddey · F. T. Ciacchi
CSIRO Manufacturing and Infrastructure Technology,
Private Bag 33, Clayton South 3169,
Victoria, Australia
e-mail: Sukhvinder.Badwal@csiro.au

than 80%, with zero greenhouse gas and pollutant emissions at end-use sites with water as the only by-product. Hydrogen can be alternatively used as a fuel in an internal combustion engine, for example, in a car to power the mechanical drive train.

Several technologies are under development for hydrogen generation including:

- Reforming fossil fuels (natural gas, liquified petroleum gas, gasoline, diesel, coal, methanol, etc.) with appropriate fuel processing/cleaning
- Electrolysis of water (energy source: nuclear, fossil, renewable)
  - Low-temperature (alkaline and polymer electrolyte membrane, PEM) and
  - High-temperature ceramic membranes
- Hybrid fossil fuel/renewable technologies (e.g. solar thermal reforming)
- Biomass gasification
- Photo-electrochemical/photo-catalytic splitting of water
- Thermolysis of water
- Thermo-chemical processes

Photo-electrolysis is considered to be an ideal prospect for hydrogen generation using only sunlight. However, the technology is in the early stages of research on materials development. There are substantial technical challenges related to efficiency, cost and lifetime. It is a long way away from meeting the collective technical and commercial targets for hydrogen production [5, 6]. There are other issues such as the logistics of hydrogen collection from large surface areas (small current densities for hydrogen production). Other proposed technologies such as thermolysis and thermochemical processes suffer from severe material-related problems [5, 6].

Although in the short to medium term, increased hydrogen demand is likely to be met by fossil fuels (e.g. natural gas reforming, coal gasification with $CO_2$ separation/sequestration), in the medium to long term, renewable energy offers the best possible solution. With time, the use of renewable energy (solar, wind, tidal, wave, etc.) as a clean alternative power is likely to increase as the cost of production declines. These renewable sources are intermittent sources of power. In the absence of energy storage, these renewable systems have to be grossly over-designed in terms of capacity. Hydrogen offers the flexibility of energy storage for long duration.

Hydrogen can be easily produced from water by electrolysis using intermittent renewable energy and off-peak electricity from nuclear, hydro or thermal power plants. Water electrolysis is considered to be one of the key technologies for hydrogen generation as it is compatible with existing and future power generation technologies and a large number of renewable technologies (solar, biomass, hydro, wind, tidal, wave, geothermal, etc.). In particular, hydrogen enables the long-term storage of energy for load levelling.

The major advantages of producing hydrogen via this route are that the technology is relatively more mature compared to other technologies such as direct water splitting (photo-electrochemical), biological routes, etc., and the electrical/water infrastructure already exists. On-site hydrogen generation can reduce the need for up-front expensive hydrogen transmission/distribution infrastructure. The major issues associated with large-scale adoption of the electrolysis technology are the high capital cost of the electrolyser (>A$5,000/kW), low system efficiencies, lifetime performance and integration with renewable sources [5, 6].

In this paper, developmental work on solid state water electrolysis technology based on polymer electrolyte membrane for small-scale distributed hydrogen generation has been described. Small-scale distributed production of hydrogen will enhance its availability at consumer level (transport, distributed generation, fuelling of micro devices, etc.) without the cost of large hydrogen distribution and storage facilities. It will, therefore, accelerate the hydrogen economy by providing local hydrogen at more attractive investment costs. PEM-based electrolysis systems offer a number of attributes such as modular aspect (there is minimal penalty on efficiency due to unit size), all solid state system (no alkaline liquid electrolytes or its recycling involved and water and electricity are the only inputs required), pure hydrogen and oxygen generation (due to physical separation by solid electrolyte membrane), ability to produce hydrogen at a pressure (electrochemical compression), small footprint due to high current densities achievable (>1 A $cm^{-2}$ as compared to ~0.4 A $cm^{-2}$ by alkaline system) [7–9]. PEM electrolysis technology due to its fast response time and start-up/shut-down characteristics (hydrogen generation starts immediately at ambient conditions) and ability to accept large variations in load is ideal for integration with intermittently available sources of electricity (renewable and off-peak grid). In addition, due to the similar aspects of the PEM electrolysis and fuel cell technologies, the impact on development and system cost reduction can be enormous.

## Experimental procedures

### Electrolysis cell/stack construction

Membrane electrode assemblies (MEAs) for water electrolysis varying in dimension from 9 up to 150 $cm^2$ active electrode area and stacks up to multi-kilowatts equivalent hydrogen generation capacity were constructed for evaluation as described below. The hydrogen electrode of the cells was prepared using Pt/C catalyst with platinum loadings of up to 0.4 mg·$cm^{-2}$ as detailed elsewhere [10]. The oxygen electrode was prepared using various noble metal catalysts with loading in the 0.2–0.4 mg·$cm^{-2}$ range on a metallic support. The polymer electrolyte membranes used were Nafion N112 and N115. Membrane electrode assemblies for electrolysis cells were prepared by hot pressing the membrane between the hydrogen and oxygen electrodes. Metallic plates with parallel cross channel flow fields were used as interconnects. The electrolysis cells

with interconnect plates were stacked and assembled with the end interconnects on both sides of the stack, serving dual functions—as interconnects as well as current collectors for the stack.

Several single cells or stacks with 50, 100 and 150 $cm^2$ active area per cell were fabricated and assembled to investigate the issues related to cell scale-up, stacking, performance, degradation and lifetime. Stack modules ranging in hydrogen generation capacity from 100 $W_{H2}$ to 2 $kW_{H2}$ were constructed and evaluated. For the 9 $cm^2$ cells and 50 $cm^2$ stacks, Nafion membrane N112 (50 μm thick) was used whereas for the 100 $cm^2$ stacks, thicker Nafion membrane N115 (125 μm thick) was used.

### Cell and stack evaluation

Test stations with built-in diagnostic tools were constructed in-house with multiple levels of operator and stack safety redundancy and capability to test electrolysis cells/stacks up to 5 $kW_{H2}$ capacity. One test station was constructed to operate stacks to 20 barA pressure. The system design allows for a continuous unattended operation of the electrolysis cells/stacks for extended periods of time with continuous monitoring of voltages of individual cells and stacks, stack current and water temperatures in different parts of the flow circuit. All key operator safety and stack safety system components (vent pressure, gas and temperature sensors, low water level and flow switches) are interlocked with the power source to stop the hydrogen/oxygen generation in the event of hydrogen leak or any other safety-related issues.

For screening and evaluation of electrolysis cell materials, design parameters and operating conditions, cells of 9 $cm^2$ active area, were used. Cells of this size were also used for electrochemical diagnostic analysis as even a small current signal can produce reasonably high current densities. The small cells (9 $cm^2$) were operated at different temperatures between room temperature and 80°C to determine the optimum operating temperature. The cell temperature was maintained with external heating. The effect of catalyst loading, membrane thickness and interface modification on the cell performance was studied at a typical cell operating temperature in the 75–85°C range.

Electrochemical investigations included current–voltage characteristics, electrochemical impedance spectroscopy on selected cells, efficiency calculations and performance degradation as a function of time at current density of 1 A $cm^{-2}$. The hydrogen generation efficiency was calculated based upon thermo-neutral voltage, $V_{thn}$, of 1.48 V [11]. Current efficiency was determined by measuring the hydrogen gas flow exiting and that expected for a given charge flow.

Stack testing involved determining current–voltage curves at different operating times of its operation, current efficiency, overall stack hydrogen generation efficiency, lifetime testing, operation in a thermally self-sustaining mode (no supplementary heating of water) and evaluation of the degradation mechanisms.

Impedance spectroscopy was performed with the Zahner model IM6e over the frequency range of 0.1 Hz to 1 kHz at 75°C on selected 9 $cm^2$ active area cells at the start and after operation of the cell for different times at a current density of 1 A $cm^{-2}$. The software package Thales provided by Zahner was used for data acquisition and fitting of the data to a simple equivalent circuit consisting of a series resistor representing all ohmic losses in the cell in series with constant phase angle element in parallel with a resistor representing the electrode/electrolyte interface, after correcting the data for lead resistance and measuring circuit parameters.

## Results and discussion

### Single cells

Several single cells of 9 $cm^2$ active electrode area, with different catalysts, loadings, membrane type and thickness, interface modification, oxygen electrode support material, etc., were investigated. Figure 1 shows typical voltage–current characteristics and efficiencies as a function of current density of a 9 $cm^2$ active area cell operating at 75°C. The cell produced efficiencies of 82% at 1 A $cm^{-2}$ and 69% at 2 A $cm^{-2}$, respectively. It should be noted that there is no oxygen or hydrogen generation below the thermo-neutral voltage of 1.48 V. There is almost a linear relationship between voltage and current once the current starts flowing through the cell but more specifically above 0.5 A $cm^{-2}$. It is worth noting that this linear relationship continues even up to 2 A $cm^{-2}$ current density with no sign of limiting currents (due to diffusion limiting processes). These results indicate that most of the voltage losses across the MEA are ohmic in nature (the membrane, electrode supports, electrode materials (anode and cathode) and contact resistances). The polarisation losses appear to be relatively small. The surface-specific resistance value determined from this linear relationship at current densities above 0.5 A $cm^{-2}$ was 0.335 Ω $cm^2$.

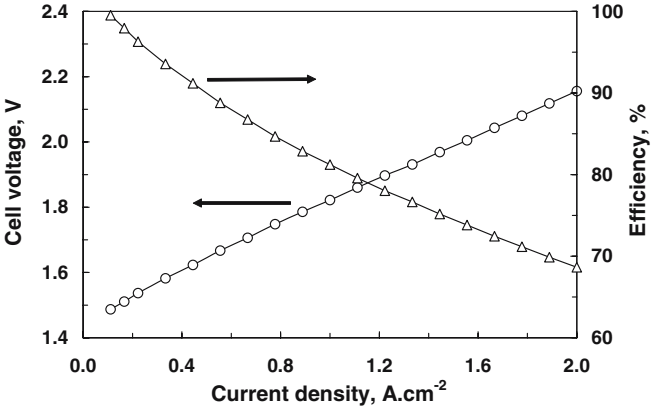


**Fig. 1** Voltage–current characteristics (○) and efficiencies (△) of a 9 $cm^2$ active area electrolysis cell (Nafion membrane N112, 50 μm thick) operating up to 2 A $cm^{-2}$ current density. Data were recorded at 75°C

In general, higher performance was achieved with thinner membranes (50 μm). However, such membranes are found to be more fragile, have short lifetime and need to be handled very carefully. There is also a complex relationship between catalyst loading, the method of catalyst deposition, performance and lifetime. The three phase boundary area between the reactant species, electrode and electrolyte need to be optimised to reduce catalyst loading, attain high hydrogen generation efficiency and increase lifetime.

## Scale-up and stack evaluation

The electrolysis cells of sizes 50 and 100 $cm^2$ active areas were fabricated and stacks of varying capacity assembled to investigate the issues related to scale-up and stacking. Figure 2 compares the *V–I* characteristics of 9 $cm^2$ active area single cell, 50 $cm^2$ active area three-cell and six-cell stacks, and 100 $cm^2$ active area two-cell and 14-cell stacks $(2kW_{H_2})$. In the case of stacks, Y-axis represents average voltage per cell in the stack. The horizontal lines in the figure have been drawn at cell voltages corresponding to 80, 85 and 90% efficiencies. The data in this figure shows a significant improvement in efficiencies of 50 and 100 $cm^2$ stacks as compared to 9 $cm^2$ active area single cells. Furthermore, the figure shows that, at 1 A $cm^{-2}$ current density, the efficiency of the 50 $cm^2$, six-cell stack is 87% as compared to 84% for the three-cell stack, and the efficiency of the 100 $cm^2$, 14-cell stack is 86% as compared to 83% for the two-cell stack. These results indicate that the increase in number of cells in the stack improves the efficiency of the stack. It appears that increasing the number of cells in the stack results in a more uniform temperature distribution and also lower average contact resistance per cell (higher ohmic losses are expected for end cells and at current collection plates). This is also reflected in the area-specific resistances calculated from the *V–I* curves (0.21 Ω $cm^2$ for the 50 $cm^2$ six-cell stack and 0.27 Ω $cm^2$ for the 100 $cm^2$, active area 14-cell stack). It should be noted that for the 9 $cm^2$ cells and 50 $cm^2$ stacks, Nafion membrane N112 (50 μm) was used, whereas for the 100 $cm^2$ stacks, thicker Nafion membrane N115 (125 μm) was used and, thus, somewhat higher specific resistance. The relationship between current and voltage is again reasonably linear for all cells and stacks above the current density of 0.5 A $cm^{-2}$ indicating the major contribution from ohmic resistance within the stack.

The 14-cell stack generated about 11 l/min of hydrogen and 5.5 l/min of oxygen at an initial efficiency of over 85% at 1 A $cm^{-2}$ (Fig. 3). This stack was first operated without any insulation but with an auxiliary heater supplying hot water at 80°C for electrolysis. The stack was subsequently operated at different current densities without any supplementary heating in a thermally self-sustaining mode with input water at room temperature (22°C). The results are shown in Fig. 4. As the current was slowly increased to 100 A (1 A $cm^{-2}$), within a few minutes, the stack reached its maximum operating temperature with the temperature of

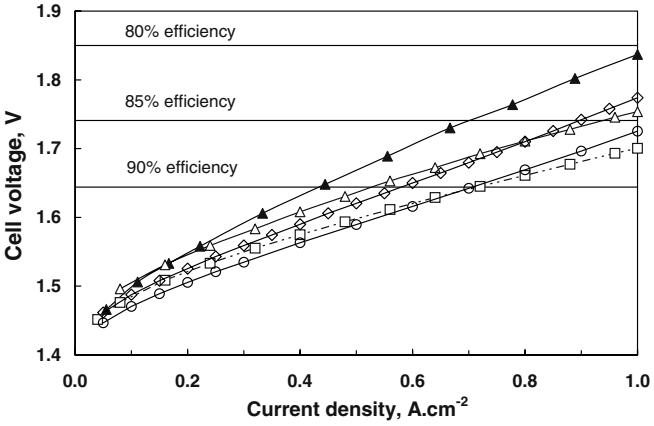


**Fig. 2** Voltage–current characteristics of electrolysis cells showing the technology scale-up from 9 to 100 $cm^2$ active area cells and from single cells to a 14-cell stack. In the case of stacks, the data have been normalised to a single cell voltage. In all cases, data were recorded at 80°C except the 9 $cm^2$ cells for which data were recorded at 75°C. ▲, 9 $cm^2$ active area single cell; △, three-cell stack with 50 $cm^2$/cell active area; □, six-cell stack with 50 $cm^2$/cell active area; ◇, two-cell stack with 100 $cm^2$/cell active area; ○, 14-cell stack with 100 $cm^2$/cell active area

the water exiting the stack of 85–86°C. This may have been even higher had the stack been insulated. At 80 A (0.8 A $cm^{-2}$) current flow, the temperature of the water exiting the stack was 80°C, at 60 A (0.6 A $cm^{-2}$) it was 73°C and at 50 A (0.5 A $cm^{-2}$) it was 67°C. It is clear that a significant amount of heat is generated within the stack due to internal resistive losses, which is sufficient to keep the stack in a thermally self-sustaining mode. The final stack temperature would be determined by the internal cell losses within the stack, current density, level of stack insulation or losses to the surroundings and the water flow rate.

## Current or Faradaic efficiency

The current efficiency was measured by relating the flow rate measurements (the amount of hydrogen generated per unit time) with the current flow per unit time. Most of the cells showed near 100% Faradaic efficiency during oper-

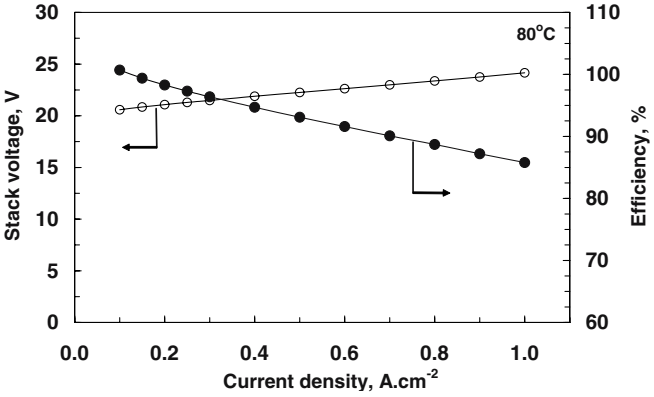


**Fig. 3** Voltage–current characteristics (○) and efficiencies (●) obtained from a 2 kW hydrogen equivalent electrolysis stack (Nafion membrane N115, 125 μm thick)

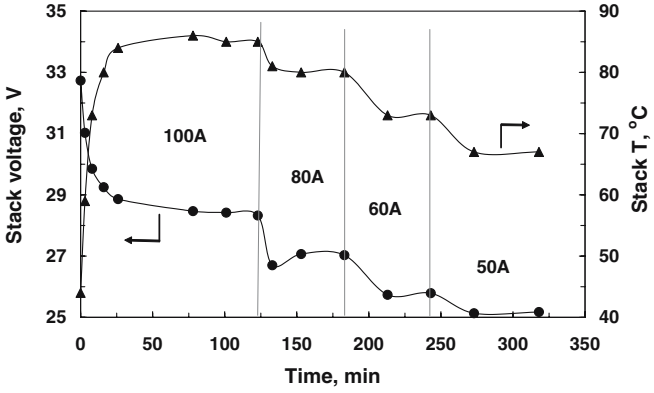


**Fig. 4** The operation of the 14-cell (100 $cm^2$ per cell active area), 2 kW hydrogen equivalent stack in a thermally self-sustaining mode. The stack voltage (●) and stack temperature (▲) are plotted as a function of time for different current values

ation. However, over a period of operation, some cells from time to time developed internal electronic short circuits which led to a drop in the current efficiency, as discussed in the next section.

## Lifetime performance and degradation mechanism

A 50 $cm^2$ active area four-cell stack with Nafion membrane N115 $(0.25kW_{H_2})$ has been operated at 1 A $cm^{-2}$ current density for lifetime performance evaluation for a period of more than 1,500 h at 80°C. The hydrogen and oxygen gases were generated at atmospheric pressures. The stack was usually operated continuously during weekdays for approximately 100 h and shut down over the weekends. Figure 5 shows the lifetime performance data of the stack in terms of stack voltages at the start ($E_s$) and after 6 h ($E_6$) of continuous operation into the 100 h cycle to simulate the operation of the electrolyser with an intermittent source of energy such as solar photovoltaic. Up to 400 h of operation, the stack efficiency was between 80 and 85%. The data also shows that there is about 3% drop in the stack efficiency during the 6 h operation, and about 2.5% of this is recovered at the start of the next cycle of operation. The average rate of drop in the stack efficiency during 1,500 h of operation was 1.30% and 1.04% per 100 h of operation for $E_s$ and $E_6$, respectively. There are several possible reasons for this degradation in performance, such as an increase in the contact resistance between the oxygen electrode support and the interconnect due to surface oxidation, changes in interfacial conditions (de-bonding of electrode/membrane, changes in catalyst surface/structural properties), membrane conductivity loss due to contamination from other ionic species entering the water sub-circuit, etc. The temporary (recoverable) drop in efficiency of the stack appears to be related to charging/discharging of the interface, saturation of the water with oxygen and/or adsorption of oxygen molecules on the reaction sites. Preliminary electrochemical impedance studies on 9 $cm^2$ active area single cells indicate an increase in ohmic losses ($R_{el}$, the left intercept of the respective arc on the real impedance axis) with time with very little effect on the electrode resistance, $R_p$, the difference of the intercepts of the respective arc on real impedance axis (Fig. 6). The impedance data were recorded at the start of the operation and after 170 h of hydrogen and oxygen generation at a current density of 1 A $cm^{-2}$. Further electrochemical tests, interconnect surface examination and membrane electrode assembly analysis are being carried out, in addition to monitoring pH and conductivity of water at various locations in the water supply sub-circuit, to understand the exact mechanisms of this cell/stack degradation.

Another catastrophic degradation has also been observed for cells that have been operated for long periods of time (typically >1500 h). This, in fact, is related to internal electronic short circuiting through the electrolyte membrane and loss of Faradaic efficiency as discussed below.

For a normal cell with near 100% current efficiency (that is, all the current that flows in the cell goes towards hydrogen and oxygen generation), no current flows in the cell up to the thermo-neutral cell voltage of about 1.48 V (Fig. 7) [11]. Above this voltage, the behaviour is that shown by the near-linear portion of the voltage–current plot (○, Fig. 7), recorded after 1,728 h of accumulated operation at a current density of 1 A $cm^{-2}$ and at 80°C. However, after 1,782 h of accumulated operation at 1 A $cm^{-2}$, it was observed that the current flowed through this cell even at voltages below 1.48 V (▵, steeper section in Fig. 7). Such cells also showed lower current efficiency (the amount of hydrogen generated for the electric charge flow was lower than that expected theoretically). It is believed that this behaviour is caused by physical damage to the membrane over a period of operation at high current densities and internal short circuiting of the membrane. However, the electronic short circuit paths initially still have quite high resistance and the voltage across the cell can reach 1.48 V at relatively low current densities. Once this

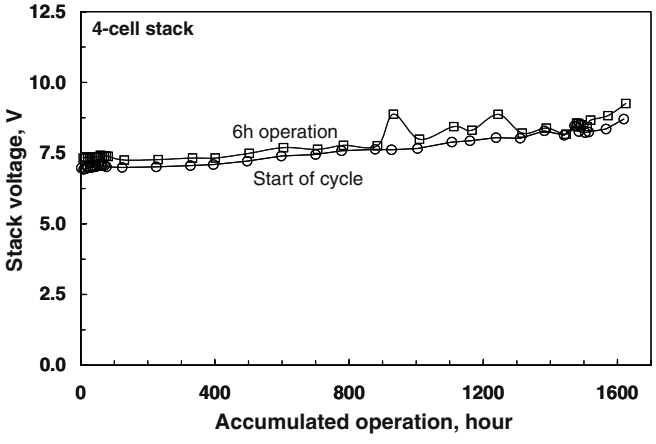


**Fig. 5** Lifetime performance data for a 0.25 kW hydrogen equivalent four-cell (50 $cm^2$ per cell active area) electrolysis stack (Nafion membrane N115, 125 μm thick). ○, voltage data at the start of the hydrogen generation cycle at 1 A $cm^{-2}$ current density and □, after 6 h of continuous operation to simulate the solar PV cycle. Data were recorded at 80°C

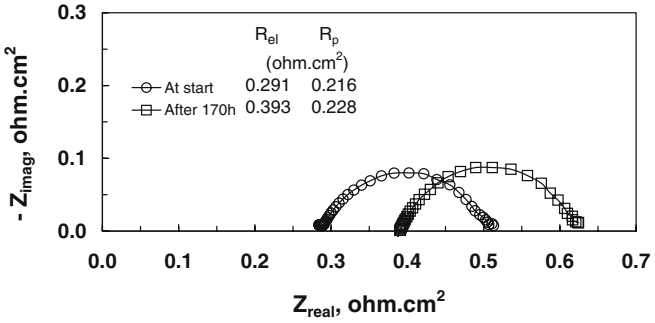


**Fig. 6** Impedance diagram (real impedance, $Z_{real}$) vs imaginary impedance ($Z_{imag}$) for a 9 $cm^2$ electrolysis cell (Nafion membrane N112, 50 μm thick) operating at 75°C, showing increase in ohmic losses with time. ○ at the start and □ after 170 h of operation at 1 A $cm^{-2}$ current density

threshold voltage is reached, part of the current goes towards hydrogen generation and the cell behaviour is that shown in the less steep section of the 1,782 h plot (△, Fig. 7). This electronic current flow is responsible for the loss of current or Faradaic efficiency. An optical examination of some damaged cells indeed confirmed membrane rupture.

To further understand this behaviour, we have tried to qualitatively model the overall cell behaviour in terms of electrical equivalent circuits shown in Fig. 8. Circuit 1 in the figure can be used to describe the behaviour observed when there is no internal short circuiting of the membrane and the current efficiency is near 100%. No current flows through the cell when the applied voltage is below 1.48 V represented by $V_{thn}$ in circuit 1. Once the applied voltage exceeds the thermo-neutral voltage, the current starts flowing through the cell and almost a linear voltage current relationship is observed as shown in Fig. 7 (○).

For the case when there is an electronic short through the membrane, circuit 2 in Fig. 8 can be used to describe the

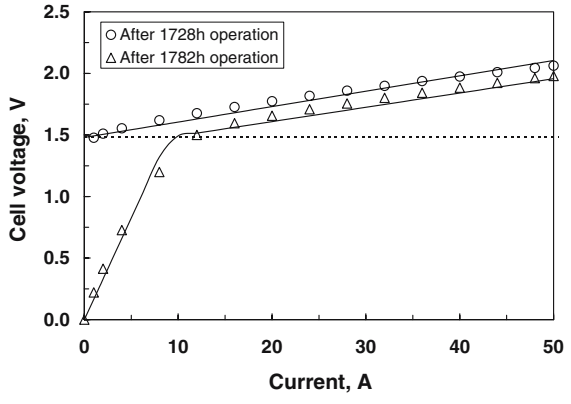


**Fig. 7** Voltage–current characteristics of a cell in the four-cell (50 $cm^2$ per cell active area) electrolysis stack (Nafion membrane N115, 125 μm thick) after 1,728 and 1,782 h (○ and △, respectively) operation at 1 A $cm^{-2}$ current density and 80°C. The *solid lines* are fitted data as per models described in Fig. 8 ($R_p$+$R_{el}$=0.0125 Ω for the 1,728 h fitted curve and $R_p$+$R_{el}$=0.0125 Ω and $R_{short}$=0.165 Ω for the 1,782 h fitted curve). The *dotted line* has been drawn at the thermo-neutral voltage of 1.48 V [11]

observed behaviour (△, Fig. 7). When the cell voltage is below 1.48 V, the current initially flows through electronic short circuit paths in the membrane and there is no ionic current flow and, thus no hydrogen generation occurs. With increasing applied voltage, more and more current flow through these short circuit paths represented collectively by $R_{short}$ [consisting of a number of resistors ($R_{s1}$, $R_{s2}$–$R_{sn}$) in parallel]. Once the applied voltage exceeds 1.48 V, part of the total current starts flowing as ionic current and it goes towards hydrogen and oxygen generation. We have fitted the data in Fig. 7 to the equivalent circuit models and equations given in Fig. 8 (○, circuit 1 and △, circuit 2) and derived the values of 0.0125 Ω for $R_p$ (the polarisation resistance at the electrode/electrolyte interface) plus $R_{el}$ (representing the total ohmic losses in the cell) for both sets of data, and the value of 0.165 Ω for $R_{short}$ for the data represented by △ in Fig. 7. The solid curves in Fig. 7 are the fitted data and show an excellent fit to the experimental data.

For fitting the data to these circuit models, we have made the following assumptions: The major voltages and efficiency losses across the cell are ohmic in nature (electrolyte membrane, support materials, current collection plates and contact resistances) with relatively low contribution from polarisation losses at interfaces between electrodes and the electrolyte as obvious from the near-linear voltage–current relationship above 1.48 V. It should be noted that, in general, the major efficiency losses in electrolysis cells occur as a result of activation polarisation and ohmic resistance, with insignificant contribution from concentration polarisation effects. However, it has been reported and as indeed also observed in the present work that ohmic losses are much higher compared to activation polarisation losses especially for higher current densities [12, 13].

We have also assumed that, at least during the collection of *V–I* data, $R_{short}$ remains reasonably constant. This assumption may, however, be somewhat flawed as it will be shown later that, once there is an electronic short through the membrane, the cell degradation at higher current densities increases more rapidly with time and it is possible that during collection of the current voltage curve, $R_{short}$ may have changed slightly.

In Fig. 9, values of total ($I_t$), short circuit ($I_{short}$) and Faradaic or ionic ($I_{Faradaic}$) currents have been plotted as a function of the applied voltage. These results show that although the cell had developed electronic conductivity, it would still generate hydrogen once the voltage across the cell exceeds 1.48 V. For example, at a current density of 1.0 A $cm^{-2}$, about 76% of the current flowed through the cell as ionic current or part of the current that contributed to the hydrogen and oxygen generation. However, it was observed that, once electronic short circuiting occurred through the electrolyte membrane, the slope of the initial part of the curve decreased with time of the current passage, indicating lower $R_{short}$ values and, thus, increased electronic short circuit paths. Typical behaviour is shown in Fig. 10 for a cell which had developed electronic short circuiting. The plots after 1,644 and 1,650 h (○ and ●, respectively) of current passage at 1.0 A·$cm^{-2}$ current

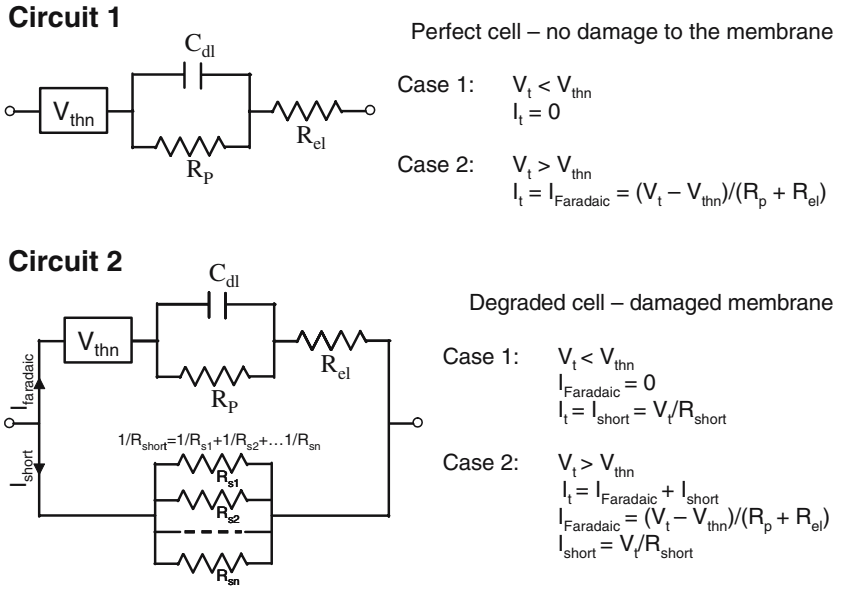


**Fig. 8** Equivalent circuit representation of a normal cell (no internal short circuiting), circuit 1, and a damaged cell with internal electronic short through the membrane, circuit 2. $I_t$=total current flowing through the circuit; $I_{Faradaic}$=Faradaic current which goes towards hydrogen and oxygen generation; $I_{short}$=short circuiting current responsible for loss in hydrogen generation efficiency; $R_p$= polarisation resistance (activation and concentration) at the electrode/electrolyte interface; $C_{dl}$=double layer capacitance at the electrode/electrolyte interface; $R_{el}$=total ohmic losses consisting of resistance of electrolyte membrane, support materials, current collection plates and contact resistances; $R_{short}$=total short circuit resistance consisting of a number of parallel short circuit resistors ($R_{s1}$, $R_{s2}$—$R_{sn}$), each representing a short circuit path through the membrane; $V_t$=total voltage drop across the cell; and $V_{thn}$thermo-neutral voltage [11]

density clearly show a decrease in the value of $R_{short}$ with increased time of current passage.

## Technology demonstration

There is substantial market for small-scale distributed hydrogen generation. PEM electrolysis technology, due to its fast response time and start-up/shut down characteristics and ability to accept large variations in load, has the potential for coupling with intermittent sources of renewable electricity with minimal power electronics. Thus, it is important to investigate the response of the PEM electrolyser to an intermittent and variable power source and its effect on the electrolyser performance and efficiency over a period of time. As hydrogen offers the flexibility of energy storage for long duration, the PEM electrolyser technology will be demonstrated as a remote area power supply as shown in a conceptual diagram (Fig. 11) in a totally sustainable energy cycle.

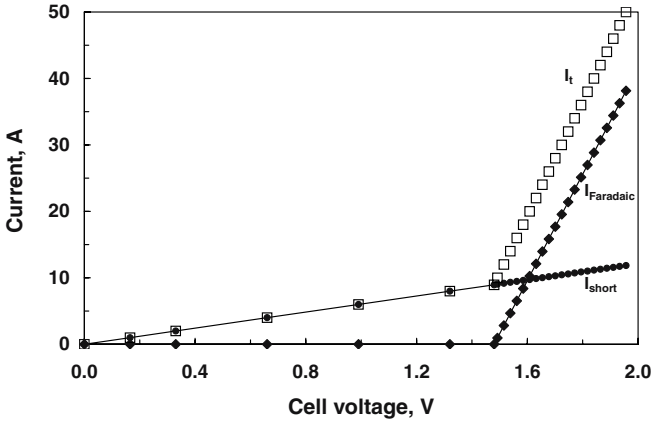


**Fig. 9** Plots of total (□), Faradaic (◆) and short (●) circuit currents vs cell voltage calculated from parameters derived for the fitted curve to the 1,782-hour operation data in Fig. 7 and as per the model equivalent circuit 2 in Fig. 8

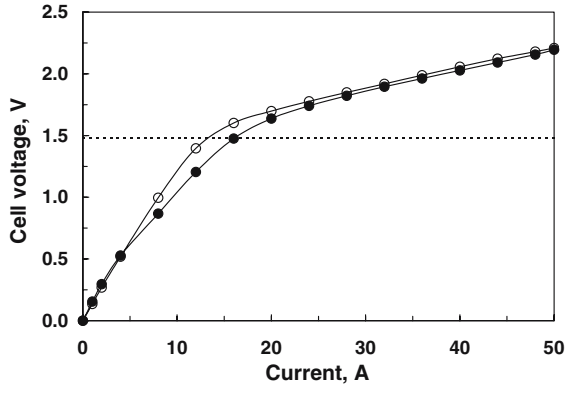


**Fig. 10** Voltage–current characteristics of a cell in the four-cell (50 $cm^2$ per cell active area) electrolysis stack (Nafion membrane N115, 125 μm thick) after 1,644 and 1,650 h (○ and ●, respectively) operation at 1 A $cm^{-2}$ current density and 80°C, showing rapid increase in cell degradation and increased electronic short circuit paths after initial onset of electronic short circuiting of the electrolyte membrane

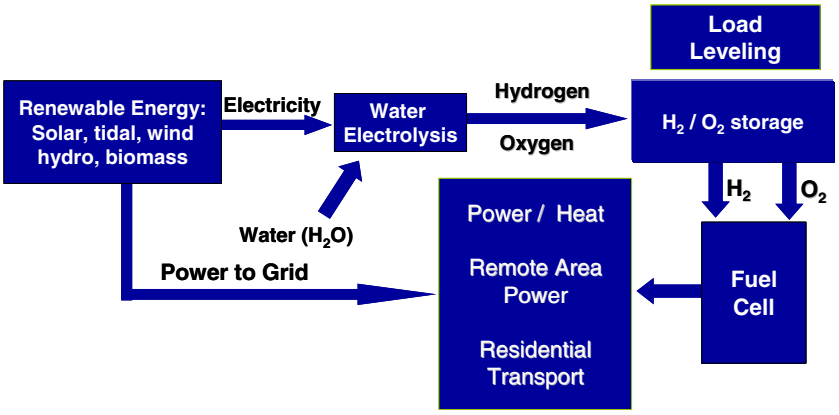


**Fig. 11** Concept diagram for demonstration of the electrolysis technology in a sustainable energy cycle as a remote area power supply

## Conclusions

Electrolysis cells have been scaled from 9 to 150 $cm^2$ active area with very little loss in hydrogen generation efficiency. Test stations to test stacks to 5 $kW_{H2}$ capacity and pressures to 20 barA have been constructed with multiple levels of safety redundancy. The system design allows for an unattended safe operation of stacks for extended periods. Stacks of varying dimensions and hydrogen generation capacity have been built and tested, some for periods exceeding 1,500 h at a current density of 1 A $cm^{-2}$. Efficiency of up to 87% initially at 1 A $cm^{-2}$ has been achieved through optimisation of interface, catalyst, MEA fabrication, fluid/current flow and stack design. The largest size stack tested to date has hydrogen generation capacity of 11 l/min and oxygen generation capacity of 5.5 l/min. The operation of this stack has been demonstrated in a thermally self-sustaining mode from cold start with water and electricity as the only inputs. Temperatures exceeding 80°C can be easily achieved at a current density of 0.8 A $cm^{-2}$ or higher. Causes of degradation have been discussed and the major cause of hydrogen generation efficiency loss has been established to be the electronic short circuiting through the polymer membrane. The results have been explained in terms of electrical equivalent circuit models. Future work, apart from optimisation of stack components and system design, is to reduce cost and performance degradation. It would also involve demonstration of the technology initially as a remote area power supply by mapping the total available solar or wind power for a site on a yearly basis and matching this with daily, weekly and yearly power demand and hydrogen generation and storage requirements.

**Acknowledgements** The authors would like to thank Kristine Giampietro and Pon Kao for their assistance with the experimental work. The manuscript was reviewed by Robin Clarke and Pon Kao. The work described in this paper forms part of CSIRO's Energy Transformed Flagship research program into positioning Australia for a future hydrogen economy.

## References

1. International Atomic Energy Agency (1999) Hydrogen as an energy carrier and its production by nuclear power. Report IAEA TECDOC-1085. Available at http://www-pub.iaea.org/MTCD/publications/PDF/te_1085_prn.pdf
2. Campbell CJ (2002) World: oil and gas industry-peak oil: an outlook on crude oil depletion. Revised, February 2002, http://www.mbendi.com/indy/oilg/p0070.htm
3. Campbell CJ, Leherrère JH (1998) The End of Cheap Oil. Scientific American, March 1998, 6 pp
4. Duncan RC, Youngquist W (1998) The world petroleum life cycle. PTTC workshop on OPEC oil pricing and independent oil producers. Petroleum Technology Transfer Council, October 1998, http://www.dieoff.com/page133.pdf
5. US DOE. Energy efficiency and renewable energy, hydrogen fuel cell and infrastructure technologies program, multi-year research, development and demonstration plan: planned program activities for 2003–2010, technical plan—hydrogen production, http://www.eere.energy.gov/hydrogenandfuelcells/mypp/pdfs/production.pdf. US DOE hydrogen, fuel cells and infrastructure technologies program review proceedings 2004 and 2005. Available at http://www.eere.energy.gov/hydrogenandfuelcells/2004_annual_review.html and http://www.hydrogen.energy.gov/annual_review05_proceedings.html
6. McHugh K (2005) Hydrogen production methods. February 2005, MPR-WP-0001, MPR Associates, Alexandria, Virginia, USA
7. Millet P, Andolfatto F, Durand R (1996) Design and performance of a solid polymer electrolyte water electrolyzer. Int J Hydrogen Energy 21:87–93
8. Friedland RJ, Speranza AJ (1999) Integrated renewable hydrogen utility system. Proceedings of the 1999 US DOE Hydrogen Program Review, NREL/CP-570-26938
9. Prince-Richard S, Whale M, Djilali N (2005) A techno-economic analysis of decentralized electrolytic hydrogen production for fuel cell vehicles. Int J Hydrogen Energy 30:1159–1179
10. Giddey S, Ciacchi FT, Badwal SPS (2004) Design, assembly and operation of polymer electrolyte membrane fuel cell stacks to 1 $kW_e$ capacity. J Power Sources 125:155–165
11. Onda K, Kyakuno T, Hattori K, Ito K (2004) Prediction of production power for high-pressure hydrogen by high-pressure water electrolysis. J Power Sources 132:64–70
12. JO'M Bockris (1980) Energy options. Wiley, New York, p. 333
13. Ströbel R, Oszcipok M, Fasil M, Rohland B, Jörissen L, Garche J (2002) J Power Sources 105:208–215